

Erratum: SPITZER-IRS spectral fitting of discs around binary post-AGB stars.

C. Gielen^{1,*}, H. Van Winckel¹, M. Min¹⁷, L.B.F.M. Waters^{1,2}, T. Lloyd Evans³, M. Matsuura^{4,5}, P. Deroo⁶, C. Dominik^{2,7}, M. Reyniers⁸, A. Zijlstra⁹, K. D. Gordon¹¹, F. Kemper⁹, R. Indebetouw^{12,16}, M. Marengo¹³, M. Meixner¹¹, G.C. Sloan¹⁴, A. G. G. M. Tielens¹⁵, and P. M. Woods⁹

¹ Instituut voor Sterrenkunde, Katholieke Universiteit Leuven, Celestijnenlaan 200D, 3001 Leuven, Belgium
e-mail: clio.gielen@ster.kuleuven.be

² Sterrenkundig Instituut 'Anton Pannekoek', Universiteit Amsterdam, Kruislaan 403, 1098 Amsterdam, The Netherlands

³ SUPA, School of Physics and Astronomy, University of St Andrews, North Haugh, St Andrews, Fife KY16 9SS, United Kingdom

⁴ UCL-Institute of Origins, Department of Physics and Astronomy, University College London, Gower Street, London WC1E 6BT, United Kingdom

⁵ UCL-Institute of Origins, Mullard Space Science Laboratory, University College London, Holmbury St. Mary, Dorking, Surrey RH5 6NT, United Kingdom

⁶ Jet Propulsion Laboratory, 4800 Oak Grove Drive, Pasadena, CA 91109, US

⁷ Department of Astrophysics, Radboud University Nijmegen, PO Box 9010, 6500 GL Nijmegen, The Netherlands

⁸ The Royal Meteorological Institute of Belgium, Department Observations, Ringlaan 3, 1180 Brussels, Belgium

⁹ Jodrell Bank Centre for Astrophysics, Alan Turing Building, University of Manchester, Oxford Road, Manchester, M13 9PL, United Kingdom

¹⁰ SUPA, School of Physics and Astronomy, University of St Andrews, North Haugh, St Andrews, Fife KY16 9SS, United Kingdom

¹¹ Space Telescope Science Institute, 3700 San Martin Drive, Baltimore, MD 21218, USA

¹² Department of Astronomy, University of Virginia, PO Box 3818, Charlottesville, VA 22903-0818, USA

¹³ Harvard-Smithsonian Center for Astrophysics, 60 Garden Street, MS 65, Cambridge, MA 02138-1516, USA

¹⁴ Department of Astronomy, Cornell University, Ithaca, NY 14853-6801, USA

¹⁵ Leiden Observatory, J.H. Oort Building, Niels Bohrweg 2, 2333 CA Leiden, The Netherlands

¹⁶ National Radio Astronomy Observatory, 520 Edgemont Road, Charlottesville, VA 22906, USA

¹⁷ Astronomisch Instituut Utrecht, Universiteit Utrecht, Princetonplein 5, 3584 CC Utrecht, The Netherlands

Received ; accepted

ABSTRACT

Aims. no abstract

Methods. no abstract

Results. no abstract

Key words. stars: AGB, post-AGB - stars: binaries - stars: circumstellar matter - stars: abundances - Magellanic Clouds

Recently, we have discovered an error in our Monte-Carlo spectral fitting routine, more specifically where the errors on the fluxes were rescaled to get a reduced χ^2 of 1. The rescaled errors were too big, resulting in too wide a range of 'good' fits in our 100 step Monte-Carlo routine.

This problem affects Figs. 7-9 and Table A.1-A.2 in Gielen et al. (2008), Table 3 in Gielen et al. (2009a), and Table 4 in Gielen et al. (2009b).

We corrected for this error and present the new values and errors in the tables below. The new values and errors nearly all

fall within the old error range. Our best χ^2 values and overall former scientific results are not affected. With these new errors some possible new trends in the dust parameters might be observed. These will be discussed in an upcoming paper where we extend the sample presented in Gielen et al. (2008) with newly obtained SPITZER-IRS data.

* Postdoctoral Fellow of the Fund for Scientific Research, Flanders

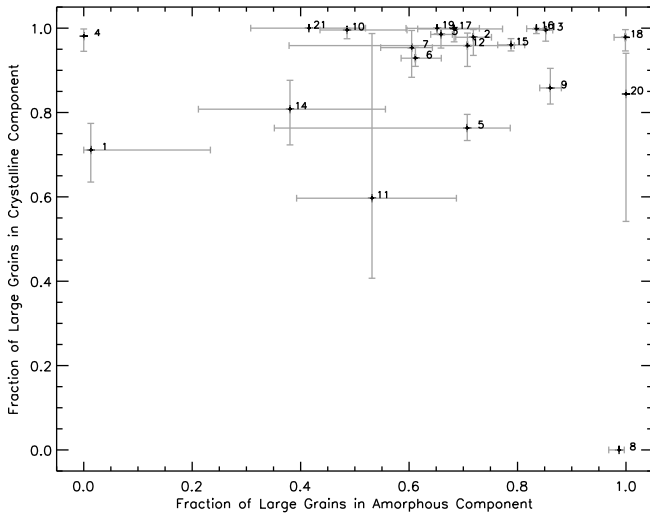


Fig. 1. Erratum for Fig. 7 in Gielen et al. (2008): The fraction of large grains in the amorphous component versus the fraction of large grains in the crystalline component, using the fitting with grain sizes of $0.1\ \mu\text{m}$ and $2.0\ \mu\text{m}$. Crystalline grains are almost completely made up of large $2.0\ \mu\text{m}$ grains.

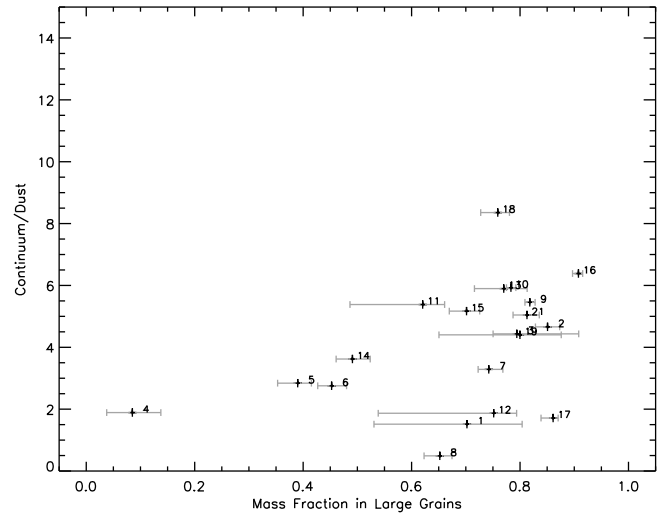


Fig. 3. Erratum for Fig. 9 in Gielen et al. (2008): The continuum-to-dust ratio of the observed spectra plotted against the mass fraction on large grains ($4.0\ \mu\text{m}$).

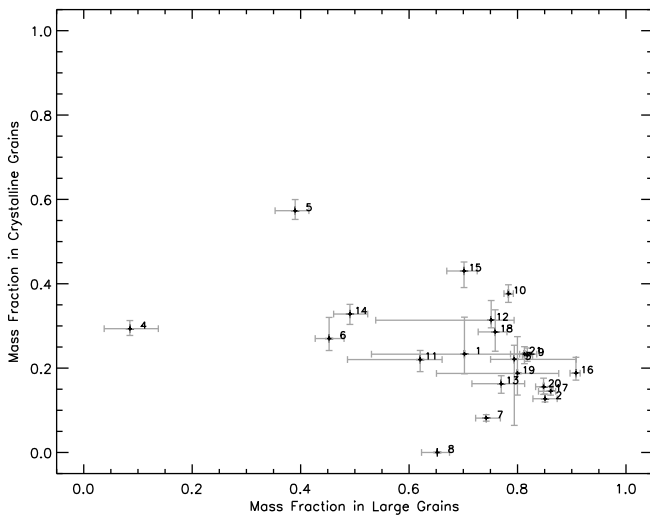


Fig. 2. Erratum for Fig. 8 in Gielen et al. (2008): The mass fraction in large grains ($4.0\ \mu\text{m}$) plotted against the mass fraction in crystalline grains, as derived from our best-fit parameters.

Table 1. Erratum for Table A.1 in Gielen et al. (2008): Best-fit parameters deduced from our full spectral fitting. Listed are the χ^2 , dust and continuum temperatures and their relative fractions.

N ^o	Name	χ^2	T_{dust1} (K)	T_{dust2} (K)	Fraction		T_{cont1} (K)	T_{cont2} (K)	Fraction	
					T_{dust1}	T_{dust2}			T_{cont1}	T_{cont2}
1	EPLyr	56.7	100 ₅₀ ⁵⁰	200 ₅₀ ⁵⁰	0.90 _{0.05} ^{0.05}	- 0.10 _{0.05} ^{0.10}	200 ₅₀ ⁵⁰	994 ₁₀₃ ⁵⁰	0.98 _{0.01} ^{0.01}	- 0.02 _{0.01} ^{0.01}
2	HD 131356	3.5	200 ₅₀ ⁵⁰	1000 ₅₀ ⁵⁰	0.90 _{0.05} ^{0.05}	- 0.10 _{0.05} ^{0.05}	200 ₅₀ ⁵⁰	500 ₅₀ ⁵⁰	0.90 _{0.01} ^{0.01}	- 0.10 _{0.01} ^{0.01}
3	HD 213985	4.4	184 ₈₇ ⁵⁰	1000 ₅₀ ⁵⁰	0.90 _{0.05} ^{0.05}	- 0.10 _{0.05} ^{0.05}	200 ₅₀ ⁵⁰	884 ₈₇ ⁵⁰	0.98 _{0.01} ^{0.01}	- 0.02 _{0.01} ^{0.01}
4	HD 52961	72.2	200 ₅₀ ⁵⁰	800 ₅₀ ⁵⁰	0.90 _{0.05} ^{0.05}	- 0.10 _{0.05} ^{0.05}	100 ₅₀ ⁵⁰	1000 ₅₀ ⁵⁰	0.99 _{0.01} ^{0.01}	- 0.01 _{0.01} ^{0.01}
5	IRAS 05208	4.5	292 ₉₅ ⁵⁰	923 ₁₁₃ ⁷⁸	0.80 _{0.10} ^{0.05}	- 0.20 _{0.05} ^{0.10}	200 ₅₀ ⁵⁰	400 ₅₀ ⁵⁰	0.85 _{0.01} ^{0.01}	- 0.15 _{0.01} ^{0.01}
6	IRAS 09060	3.6	200 ₅₀ ⁵⁰	728 ₁₃₀ ⁷³	0.90 _{0.05} ^{0.05}	- 0.10 _{0.05} ^{0.05}	228 ₁₃₀ ⁷³	834 ₂₃₇ ¹⁴¹	0.93 _{0.02} ^{0.02}	- 0.07 _{0.02} ^{0.02}
7	IRAS 09144	6.1	200 ₅₀ ⁵⁰	504 ₁₁₁ ⁵⁰	0.90 _{0.05} ^{0.05}	- 0.10 _{0.05} ^{0.05}	200 ₅₀ ⁵⁰	796 ₁₁₁ ⁵⁰	0.94 _{0.01} ^{0.01}	- 0.06 _{0.01} ^{0.01}
8	IRAS 10174	13.9	300 ₅₀ ⁵⁰	400 ₅₀ ⁵⁰	0.90 _{0.05} ^{0.05}	- 0.10 _{0.05} ^{0.05}	100 ₅₀ ⁵⁰	300 ₅₀ ⁵⁰	0.97 _{0.01} ^{0.01}	- 0.03 _{0.01} ^{0.01}
9	IRAS 16230	4.9	200 ₅₀ ⁵⁰	500 ₅₀ ⁵⁰	0.90 _{0.05} ^{0.05}	- 0.10 _{0.05} ^{0.05}	100 ₅₀ ⁵⁰	500 ₅₀ ⁵⁰	0.95 _{0.05} ^{0.05}	- 0.05 _{0.05} ^{0.05}
10	IRAS 17038	2.9	317 ₈₀ ⁸⁵	871 ₆₁ ⁸⁰	0.80 _{0.10} ^{0.10}	- 0.20 _{0.10} ^{0.10}	200 ₅₀ ⁵⁰	591 ₉₆ ⁵⁰	0.97 _{0.02} ^{0.01}	- 0.03 _{0.01} ^{0.02}
11	IRAS 17243	2.3	200 ₅₀ ⁵⁰	486 ₈₉ ⁵⁰	0.90 _{0.10} ^{0.05}	- 0.10 _{0.05} ^{0.10}	200 ₅₀ ⁵⁰	600 ₅₀ ⁵⁰	0.90 _{0.01} ^{0.01}	- 0.10 _{0.01} ^{0.01}
12	IRAS 19125	3.9	100 ₅₀ ⁵⁰	200 ₅₀ ⁵⁰	0.90 _{0.05} ^{0.05}	- 0.10 _{0.05} ^{0.05}	482 ₃₀₉ ⁵⁰	788 ₂₀₆ ⁵⁰	0.86 _{0.05} ^{0.01}	- 0.14 _{0.01} ^{0.05}
13	IRAS 19157	5.5	200 ₅₀ ⁵⁰	695 ₁₀₆ ⁵⁰	0.90 _{0.05} ^{0.05}	- 0.10 _{0.05} ^{0.05}	200 ₅₀ ⁵⁰	705 ₁₀₆ ⁵⁰	0.96 _{0.01} ^{0.01}	- 0.04 _{0.01} ^{0.01}
14	IRAS 20056	3.8	100 ₅₀ ⁵⁰	200 ₅₀ ⁵⁰	0.10 _{0.20} ^{0.10}	- 0.90 _{0.20} ^{0.10}	200 ₅₀ ⁵⁰	600 ₅₀ ⁵⁰	0.88 _{0.01} ^{0.01}	- 0.12 _{0.01} ^{0.01}
15	RU Cen	3.4	287 ₉₁ ⁵⁰	575 ₁₇₆ ⁵⁰	0.90 _{0.30} ^{0.05}	- 0.10 _{0.05} ^{0.30}	200 ₅₀ ⁵⁰	599 ₅₀ ⁵⁰	0.99 _{0.01} ^{0.01}	- 0.01 _{0.01} ^{0.01}
16	SAO 173329	3.1	200 ₅₀ ⁵⁰	702 ₅₀ ¹³⁹	0.90 _{0.05} ^{0.05}	- 0.10 _{0.05} ^{0.05}	200 ₅₀ ⁵⁰	600 ₅₀ ⁵⁰	0.93 _{0.01} ^{0.01}	- 0.07 _{0.01} ^{0.01}
17	ST Pup	8.4	200 ₅₀ ⁵⁰	500 ₅₀ ⁵⁰	0.90 _{0.05} ^{0.05}	- 0.10 _{0.05} ^{0.05}	200 ₅₀ ⁵⁰	500 ₅₀ ⁵⁰	0.95 _{0.01} ^{0.01}	- 0.05 _{0.01} ^{0.01}
18	SU Gem	1.8	154 ₅₄ ¹⁰⁵	558 ₅₉ ⁹⁶	0.80 _{0.10} ^{0.10}	- 0.20 _{0.10} ^{0.10}	200 ₅₀ ⁵⁰	800 ₅₀ ⁵⁰	0.95 _{0.01} ^{0.01}	- 0.05 _{0.01} ^{0.01}
19	SX Cen	4.3	257 ₅₈ ⁵⁰	968 ₆₉ ⁵⁰	0.80 _{0.10} ^{0.10}	- 0.20 _{0.10} ^{0.10}	200 ₅₀ ⁵⁰	691 ₉₆ ⁵⁰	0.94 _{0.01} ^{0.01}	- 0.06 _{0.01} ^{0.01}
20	TW Cam	2.3	261 ₆₂ ⁵⁰	400 ₅₀ ⁵⁰	0.60 _{0.05} ^{0.10}	- 0.40 _{0.10} ^{0.05}	100 ₅₀ ⁵⁰	500 ₅₀ ⁵⁰	0.95 _{0.01} ^{0.01}	- 0.05 _{0.01} ^{0.01}
21	UY CMa	2.9	200 ₅₀ ⁵⁰	726 ₅₀ ⁷⁶	0.90 _{0.05} ^{0.05}	- 0.10 _{0.05} ^{0.05}	200 ₅₀ ⁵⁰	500 ₅₀ ⁵⁰	0.83 _{0.01} ^{0.01}	- 0.17 _{0.01} ^{0.01}

Acknowledgements. CG and HVW acknowledge support of the Fund for Scientific Research of Flanders (FWO) under the grant G.0178.02. and G.0470.07. This work is based on observations made with the Spitzer Space Telescope, which is operated by the Jet Propulsion Laboratory, California Institute of Technology, under a contract with NASA.

References

- Gielen, C., van Winckel, H., Matsuura, M., et al. 2009a, *A&A*, 503, 843
 Gielen, C., Van Winckel, H., Min, M., Waters, L. B. F. M., & Lloyd Evans, T. 2008, *A&A*, 490, 725
 Gielen, C., Van Winckel, H., Reyniers, M., et al. 2009b, *A&A*, 508, 1391

Table 2. Erratum for Table A.2 in Gielen et al. (2008): Best-fit parameters deduced from our full spectral fitting. The abundances of small ($2.0\ \mu\text{m}$) and large ($4.0\ \mu\text{m}$) grains of the various dust species are given as fractions of the total mass, excluding the dust responsible for the continuum emission. The last column gives the continuum flux contribution, listed as a percentage of the total integrated flux over the full wavelength range.

N°	Name	Olivine		Pyroxene		Forsterite		Enstatite		Continuum
		Small - Large	Small - Large	Small - Large	Small - Large	Small - Large	Small - Large			
1	EPLyr	0.00 ^{0.00} - 0.00 ^{0.00}	15.36 ^{12.96} - 61.34 ^{10.71}	14.43 ^{4.61} - 0.02 ^{0.00}	0.00 ^{0.00} - 8.85 ^{4.49}	53.51 ^{3.36}				
2	HD 131356	0.00 ^{0.00} - 30.48 ^{1.50}	2.87 ^{1.79} - 53.91 ^{2.57}	12.06 ^{0.65} - 0.03 ^{1.00}	0.00 ^{0.00} - 0.65 ^{1.34}	76.34 ^{0.30}				
3	HD 213985	0.00 ^{0.00} - 36.08 ^{2.21}	12.58 ^{8.42} - 29.27 ^{25.84}	8.02 ^{1.63} - 7.74 ^{4.86}	0.00 ^{0.00} - 6.31 ^{2.09}	76.21 ^{0.57}				
4	HD 52961	0.00 ^{0.00} - 0.00 ^{0.00}	70.65 ^{1.61} - 0.00 ^{0.00}	20.84 ^{3.81} - 8.40 ^{5.18}	0.00 ^{0.00} - 0.12 ^{2.07}	65.66 ^{0.57}				
5	IRAS 05208	0.00 ^{0.00} - 9.52 ^{2.49}	33.16 ^{1.52} - 0.00 ^{0.00}	25.76 ^{1.34} - 0.00 ^{0.00}	2.10 ^{2.13} - 29.47 ^{2.80}	69.06 ^{0.62}				
6	IRAS 09060	0.06 ^{1.80} - 32.70 ^{4.64}	39.74 ^{3.00} - 0.48 ^{4.21}	14.95 ^{1.37} - 1.11 ^{2.97}	0.01 ^{0.40} - 10.95 ^{3.37}	72.43 ^{1.24}				
7	IRAS 09144	0.00 ^{0.00} - 39.21 ^{2.04}	17.77 ^{1.54} - 34.88 ^{7.04}	7.99 ^{0.75} - 0.00 ^{0.00}	0.00 ^{0.00} - 0.14 ^{1.21}	72.51 ^{0.39}				
8	IRAS 10174	8.70 ^{4.93} - 39.99 ^{4.24}	26.10 ^{2.29} - 25.21 ^{3.19}	0.00 ^{0.00} - 0.00 ^{0.00}	0.00 ^{0.00} - 0.00 ^{0.00}	31.48 ^{0.30}				
9	IRAS 16230	0.00 ^{0.00} - 47.54 ^{2.35}	0.00 ^{0.00} - 29.46 ^{2.01}	18.20 ^{0.90} - 4.23 ^{1.38}	0.00 ^{0.00} - 0.58 ^{1.51}	75.74 ^{0.29}				
10	IRAS 17038	0.00 ^{0.00} - 31.29 ^{2.25}	0.03 ^{0.92} - 31.02 ^{4.33}	21.65 ^{0.77} - 0.00 ^{0.00}	0.00 ^{0.00} - 16.00 ^{1.89}	81.71 ^{0.23}				
11	IRAS 17243	0.49 ^{7.03} - 42.74 ^{2.73}	20.13 ^{10.90} - 14.61 ^{5.25}	17.34 ^{0.90} - 0.00 ^{0.00}	0.00 ^{0.00} - 4.69 ^{1.76}	83.22 ^{0.41}				
12	IRAS 19125	8.22 ^{7.72} - 6.24 ^{6.47}	8.66 ^{8.00} - 45.53 ^{5.92}	7.98 ^{0.98} - 7.87 ^{1.34}	0.00 ^{0.00} - 15.50 ^{2.65}	69.72 ^{7.00}				
13	IRAS 19157	0.00 ^{0.00} - 63.21 ^{5.31}	8.43 ^{4.28} - 12.05 ^{6.89}	14.58 ^{1.36} - 0.02 ^{0.94}	0.00 ^{0.00} - 1.70 ^{2.00}	82.28 ^{0.61}				
14	IRAS 20056	0.45 ^{2.96} - 31.83 ^{3.02}	34.60 ^{3.35} - 0.30 ^{5.33}	15.86 ^{1.04} - 0.02 ^{0.85}	0.00 ^{0.00} - 16.93 ^{1.80}	83.48 ^{0.20}				
15	RU Cen	0.00 ^{0.00} - 27.92 ^{2.17}	1.24 ^{2.06} - 27.81 ^{3.82}	28.63 ^{1.83} - 3.34 ^{2.71}	0.00 ^{0.00} - 11.06 ^{2.11}	80.62 ^{0.34}				
16	SAO 173329	0.00 ^{0.00} - 52.55 ^{1.74}	0.02 ^{0.50} - 28.64 ^{2.15}	9.21 ^{1.09} - 0.02 ^{0.00}	0.00 ^{0.00} - 9.56 ^{2.63}	82.54 ^{0.44}				
17	ST Pup	0.00 ^{0.00} - 32.87 ^{1.29}	0.71 ^{1.86} - 51.93 ^{1.79}	13.19 ^{0.57} - 0.03 ^{0.83}	0.00 ^{0.00} - 1.27 ^{1.16}	54.60 ^{0.53}				
18	SU Gem	0.00 ^{0.00} - 58.69 ^{3.60}	0.70 ^{2.88} - 12.03 ^{3.93}	23.41 ^{2.31} - 2.30 ^{3.69}	0.00 ^{0.00} - 2.87 ^{3.03}	88.40 ^{0.37}				
19	SX Cen	0.00 ^{0.00} - 48.37 ^{3.30}	9.19 ^{11.44} - 23.70 ^{12.70}	10.82 ^{3.64} - 0.53 ^{2.29}	0.00 ^{0.00} - 7.39 ^{4.69}	76.16 ^{1.50}				
20	TW Cam	0.00 ^{0.00} - 84.42 ^{2.04}	0.00 ^{0.00} - 0.00 ^{0.00}	15.20 ^{1.97} - 0.00 ^{0.00}	0.00 ^{0.00} - 0.37 ^{1.84}	90.63 ^{0.15}				
21	UY CMa	0.00 ^{0.00} - 15.55 ^{2.31}	2.54 ^{2.53} - 58.59 ^{3.01}	16.18 ^{2.50} - 4.48 ^{2.93}	0.00 ^{0.00} - 2.65 ^{1.53}	78.14 ^{0.62}				

Table 3. Erratum for Table 3 in Gielen et al. (2009a): Best-fit parameters deduced from our full spectral fitting. Listed are the χ^2 , dust, and continuum temperatures and their relative fractions. Best-fit parameters deduced from our full spectral fitting. The abundances of small and large grains of the various dust species are given as fractions of the total mass, excluding the dust responsible for the continuum emission. The last column gives the continuum flux contribution, listed as a percentage of the total integrated flux over the full wavelength range.

Name	χ^2	T_{dust1} (K)	T_{dust2} (K)	Fraction $T_{dust1} - T_{dust2}$	T_{cont1} (K)	T_{cont2} (K)	Fraction $T_{cont1} - T_{cont2}$
EPLyr	5.4	100 ⁵⁰	200 ⁵⁰	0.90 ^{0.10} - 0.10 ^{0.05}	100 ⁵⁰	643 ³⁰²	0.98 ^{0.01} - 0.02 ^{0.04}
HD 52961	50.0	200 ⁵⁰	700 ⁵⁰	0.90 ^{0.05} - 0.10 ^{0.05}	100 ⁵⁰	1000 ⁵⁰	0.99 ^{0.01} - 0.01 ^{0.01}

Name	Olivine		Pyroxene		Forsterite		Enstatite		Continuum
	Small - Large	Small - Large	Small - Large	Small - Large	Small - Large	Small - Large	Small - Large		
EPLyr	0.24 ^{16.83} - 8.74 ^{7.92}	7.17 ^{13.69} - 8.09 ^{12.67}	35.18 ^{3.04} - 2.08 ^{2.61}	0.00 ^{0.00} - 38.50 ^{4.30}	57.99 ^{2.53}				
HD 52961	0.00 ^{0.00} - 0.00 ^{0.00}	59.17 ^{0.72} - 0.00 ^{0.00}	0.77 ^{1.46} - 40.06 ^{1.02}	0.00 ^{0.00} - 0.00 ^{0.00}	68.88 ^{0.46}				

Table 4. *Erratum for Table 4 in Gielen et al. (2009b):* Best-fit parameters deduced from our full spectral fitting. Listed are the χ^2 , dust, and continuum temperatures and their relative fractions. Best-fit parameters deduced from our full spectral fitting. The abundances of small ($0.1\mu\text{m}$) and large ($2.0\mu\text{m}$) grains of the various dust species are given as fractions of the total mass, excluding the dust responsible for the continuum emission. The last column gives the continuum flux contribution, listed as a percentage of the total integrated flux over the full wavelength range.

Name	χ^2	T_{dust1} (K)	T_{dust2} (K)	Fraction $T_{dust1} - T_{dust2}$	T_{cont1} (K)	T_{cont2} (K)	Fraction $T_{cont1} - T_{cont2}$
MACHO 79.5501.13	5.1	200_{50}^{50}	725_{50}^{83}	$0.90_{0.05}^{0.05} - 0.10_{0.05}^{0.05}$	346_{246}^{184}	623_{50}^{99}	$0.21_{0.18}^{0.69} - 0.79_{0.69}^{0.18}$
MACHO 82.8405.15	3.9	200_{50}^{50}	519_{75}^{82}	$0.90_{0.05}^{0.05} - 0.10_{0.05}^{0.05}$	300_{50}^{50}	500_{50}^{50}	$0.82_{0.02}^{0.03} - 0.18_{0.03}^{0.02}$

Name	Olivine Small - Large	Pyroxene Small - Large	Forsterite Small - Large	Enstatite Small - Large	Continuum
MACHO 79.5501.13	$0.00_{0.00}^{0.00} - 0.00_{0.00}^{0.00}$	$48.45_{7.00}^{4.75} - 0.37_{0.37}^{20.55}$	$0.00_{0.00}^{0.00} - 44.54_{3.32}^{3.47}$	$0.17_{0.17}^{2.86} - 6.47_{4.25}^{5.76}$	$89.27_{0.86}^{0.70}$
MACHO 82.8405.15	$0.96_{0.95}^{7.13} - 4.13_{3.97}^{10.91}$	$52.80_{9.36}^{10.75} - 4.01_{3.92}^{18.56}$	$5.50_{2.26}^{2.76} - 20.52_{7.06}^{6.47}$	$0.14_{0.14}^{3.66} - 11.95_{5.83}^{5.93}$	$82.63_{1.86}^{1.86}$